RADIATION PROPERTIES OF TAPERED HARD X-RAY FREE ELECTRON LASERS*

C. Emma, C. Pellegrini, UCLA, Los Angeles, CA, USA
J. Wu, K. Fang, S. Chen, SLAC, Menlo Park, CA, USA
S. Serkez, DESY, Hamburg, Germany

Abstract

We perform an analysis of the transverse coherence of the radiation from a TW level tapered hard X-ray Free Electron Laser (FEL). The radiation properties of the FEL are studied for a Gaussian, parabolic and uniform transverse electron beam density profile in a 200 m undulator at a resonant wavelength of 1.5 Å. Simulations performed using the 3-D FEL particle code GENESIS show that diffraction of the radiation occurs due to a reduction in optical guiding in the tapered section of the undulator. This results in an increasing transverse coherence for all three transverse electron beam profiles. We determine that for each case considered the radiation coherence area is much larger than the electron beam spot size, making coherent diffraction imaging experiments possible for TW X-ray FELs.

INTRODUCTION

Self Amplified Spontaneous Emission X-ray Free Electron Lasers (SASE X-FELs) [1–3] have been used to study structures and dynamical processes with spatial resolution of 1 Å and temporal resolution of 1 fs. This has had a particularly significant impact in the field of bio imaging where X-FELs have been used to push the frontiers of what can be done with diffraction based imaging techniques [4–6]. Future research in this field will benefit from a larger number of coherent photons/pulse, a factor of ten to one hundred larger within a pulse duration of 10-20 fs corresponding to a peak output power of 1 TW or more.

Together with high peak power, coherent X-ray diffraction imaging experiments require the radiation to be sufficiently longitudinally and transversely coherent at the sample position [7]. The longitudinal coherence can be improved by seeding or self-seeding the FEL amplifier [8–10]. Tapering the XFEL after self-seeding presents a promising solution to achieving TW power pulses with adequate longitudinal coherence. In this work we examine the transverse coherence properties of the radiation from a seeded and tapered hard X-ray FEL and determine wether the radiation is sufficiently transversely coherent to serve as an adequate source for diffraction based imaging experiments.

RADIATION PROPERTIES

FEL Radiation in a Tapered Undulator

We analyze the case of a hard X-ray tapered FEL with electron beam and undulator parameters similar to those of the LCLS-II upgrade project. The FEL is formed of

---

* Work supported by: DOE Grant Number DE-SC0009983

Table 1: GENESIS Simulation Parameters

Parameter Name	Parameter Value
Beam energy E_0	13.64 GeV
Beam peak current I_{pk}	4000 A
Normalized emittances $\epsilon_{x,n}/\epsilon_{y,n}$	0.3/0.3 μm rad
Electron bunch length l_b	16.4 fs
Peak radiation power input P_{in}	5 MW
Undulator period λ_w	32 mm
Normalised undulator parameter a_w	2.3832
Radiation wavelength λ_r	1.5 Å
FEL parameter ρ	7.361 $\times 10^{-4}$

3.4 m long undulator sections with 1m breaks for a total length of 200 m. The system is simulated using the fully 3-dmensional FEL particle code GENESIS in both single frequency and time dependent simulations (see table 1 for parameters). The magnetic field and the quadrupole focusing is optimized to yield the maximum output following the work of Ref. [11]. The simulations are performed for three different transverse electron beam distributions: uniform, parabolic and Gaussian. After the initial saturation and exponential gain regime the FEL process is dominated by refractive guiding of the radiation by the electron beam. This can be described by considering the complex refractive index of the electron beam [12]
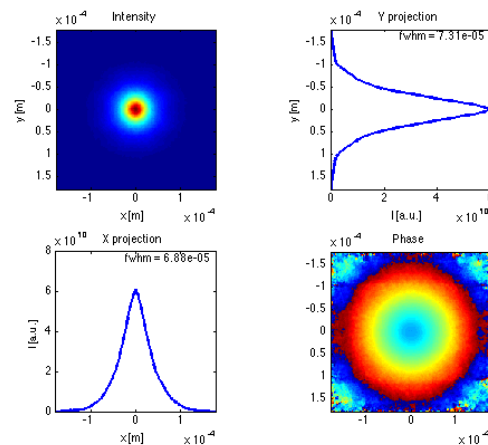
Figure 1: Amplitude and phase of the radiation field at the undulator exit (z=200 m) for a Gaussian transverse electron beam distribution obtained from time independent GENESIS simulation

Figure 2: Radiation beam size evolution (top) and spectrum (bottom) at $\lambda_r = 1.50078$ Å for a seeded hard X-ray tapered FEL at the undulator exit (z=200m) for Gaussian (green), parabolic (red) and uniform (blue) transverse electron distributions.

$$n = 1 + \frac{\omega_{p0}^2}{\omega_s^2} \frac{r_{b0}^2}{r_b^2} \frac{a_w}{2|a_s|} [JJ] \left\langle \frac{e^{-i\Psi}}{\gamma} \right\rangle \quad (1)$$

where ω_p is the electron plasma frequency, ω_s is the radiation frequency and r_b is the electron beam radius. Quantities with subscript 0 refer to initial parameters and the symbol $[JJ] = J_0(x) - J_1(x)$ for a planar undulator and $[JJ] = 1$ for a helical undulator, where $x = a_w^2/2(1 + a_w^2)$. The average term in square brackets is over the beam electrons where Ψ is the electron phase relative to the ponderomotive potential.

The electron beam microbunching $\left\langle e^{-i\Psi} \right\rangle$ decays in the tapered section of the undulator and leads to diffraction of the radiation. This is observed in time steady (Fig. 1) and time depenent simulations for a 16 fs electron bunch length at a resonant wavelength of $\lambda_r = 1.50078$ Å (see Fig. 2). For all three transverse electron distributions the radiation size increases by a factor 3-4 compared to the input seed. The effect is most enchanced for the Gaussian transverse distribution and causes an early saturation of the ouput power as discussed in Ref. [11]. The radiation spectra at $\lambda_r = 1.50078$ Å for each of the three cases are also shown in Fig. 2. The effects of the sideband instability [13, 14] on the tapered FEL cause a spectral broadening of the radiation which results in bandwidts of $\Delta\lambda/\lambda \sim 20\rho$. The flatter transverse profiles of the parabolic and uniform distributions mitigate the detrimental effects of the sideband instability more effectively. Integrating the power deposited in the
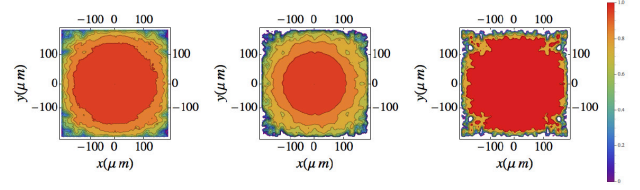
Figure 3: Modulus of the radiation complex coherence factor at the undulator exit (z=200 m). Results are shown for Gaussian (left), parabolic (center) and uniform (right) transverse electron beams and a bunch length of 16.4 fs

sidebands at $\lambda_r = 1.50078$ we notice a reduction in sideband energy of 61 % for the parabolic case and 72 % for the uniform beam as compared to the Gaussian.

Transverse Coherence

We examine the transverse coherence properties of the output radiation for the three different transverse distributions at a resonant wavelength $\lambda_r = 1.5$ Å and a bunch length of 16.4 fs. To compute the coherence area we first consider the mutual coherence function [15]:

$$\Gamma(\tau) = \left\langle \vec{E}(\vec{r_1}, t + \tau) \vec{E}^*(\vec{r_2}, t) \right\rangle \quad (2)$$

where the electric field is sampled at two transverse locations and the angle brackets denote the average over the time t. In a self-seeded tapered X-FEL we may apply the *quasimonochromatic* approximation [15] which allows us to define the mutual optical intensity function $J_{12} \equiv \Gamma(0)$. Normalization of the mutual intensity removes the amplitude information of the field and gives a measure of the phase relation between two transverse locations. This defines the complex coherence factor μ_{12}:

$$\mu_{12} = \frac{J_{12}}{\sqrt{J_{11}J_{22}}} \quad (3)$$

where $|\mu_{12}| = 0$ corresponds to vanishing transverse coherence and $|\mu_{12}| = 1$ total transverse coherence. While both the mutual intensity function and the complex coherence factor are 4-dimensional quantities we can obtain a quantitative value of the degree of coherence if we fix a single point $\vec{r_1}$ in our calculation to be the center of the beam. From μ_{12} we can then calculate the coherence area A_c:

$$A_c = \int \mu_{12} dA \quad (4)$$

The degree of transverse coherence is now quantified by computing the coherence area at various z locations in the undulator and comparing it to the radiation beam spot size. A necessary condition for diffraction imaging applications is that the coherence area be much larger than the beam spot size at the undulator exit. As can be seen by comparing the final beam sizes (Fig. 2) and the coherence areas (Fig. 3) this is indeed the case for all three transverse distributions. The coherence area grows in the tapered undulator due to diffraction of the radiation. For all three distributions at the

undulator exit the radiation beam spotsize σ_r^2 is $O(10^{-3})$ mm^2 while the calculated coherence area A_c is $O(10^{-1})$ mm^2.

CONCLUSION

We performed an analysis of the radiation properties of tapered hard X-ray FELs. The tapering strategy used was that described in Ref. [11] which maximises the output radiation power in order to reach TW level peak power or greater. The analysis was performed using the 3-dimensional particle code GENESIS in time independent and time dependent simulations. The spectral properties of the radiation were investigated for three different transverse electron beam distributions: Gaussian, parabolic and uniform. Time dependent simulations show that the radiation spectra at the undulator exit exhibit a broad bandwidth $\Delta\lambda/\lambda \sim 20\rho$. This broadening is caused by the sideband instability and is mitigated more effectively by the flatter transverse electron density profiles. Results show a reduction in sideband energy of 61 % for the parabolic case and 72 % for the uniform beam as compared to the Gaussian for a resonant wavelength $\lambda_r = 1.50078$ Å.

A quantitative study of the transverse coherence properties of the radiation from optimized X-FELs has also been carried out. Results from time dependent simulations show that the transverse coherence area A_c is larger than the beam spotsize σ_r^2 by two orders of magnitude for all electron beam transverse distributions, suggesting that the radiation from a tapered X-FEL can be used in imaging and X-ray diffraction experiments.

REFERENCES

[1] R. Bonifacio, C. Pellegrini, L. Narducci, Optics Communications, vol. 50, no. 6, p. 373, 1984

[2] J.B. Murphy, C. Pellegrini, J. Opt. Soc. Am. B, vol. 2, p. 259, 1985

[3] A. Kondratenko, E. Saldin, Part. Accel., vol. 10, p. 207, 1980

[4] M. Seibert, et al, Nature, vol. 470, p. 78, 2011

[5] H. Chapman, et al, Nature, vol. 470, p. 73, 2011

[6] J.S. Richardson, D. C. Richardson, Biophysical Journal, vol. 106, p. 510, 2014

[7] L.W. Whitehead, et. al., Phys. Rev. Lett., vol. 103, p. 103, 1009

[8] J. Feldhaus, E.L. Saldin, J.R. Schneider, E.A. Schneidmiller, M.V. Yurkov, Optics Communications, vol. 140, p. 341, 1997

[9] G. Geloni, V. Kocharayan, E. Saldin, DESY 10-053, 2010

[10] Y. Ding, Z. Huang, R.D. Ruth, Phys. Rev. ST. AB., vol. 13, 2010

[11] Y. Jiao, et. al., Phys. Rev. ST. AB., vol. 15, p. 050704, 2012

[12] D. Proznitz, A. Szoke, V.K. Neil, Phys. Rev. A., vol. 24, p. 1436, 1981

[13] T. Yang, et. al., Phys. Fluid. B, vol. 2, p. 2456, 1990

[14] R.C. Davidson, et. al., Phys. Fluid, vol. 30, p. 557, 1987

[15] J.W. Goodman, Statistical Optics, (New York, Wiley 2000), 180